Chemical Science

Accepted Manuscript

This article can be cited before page numbers have been issued, to do this please use: L. Liu, X. Chen, G. Guan, X. Su, M. Liu, Y. Hu, W. He, L. Zhang, W. Ma and K. An, *Chem. Sci.*, 2026, DOI: 10.1039/D6SC01404F.

ROYAL SOCIETY OF CHEMISTRY

rsc.li/chemical-science

View Article Online
DOI: 10.1039/D6SC01404F

ARTICLE

Rhodium-Catalyzed Enantioselective Intermolecular C–H Silylation of Simple Arenes: Synergistic Substituent Effects Overcome Silane Redistribution to Enable Synthesis of Si-Stereogenic Arylsilanes

Lichuan Liu,[a,b,†] Xingliang Chen,[a,†] Guiyu Guan,[b,†] Xinyue Su,[a] Mengqing Liu,[a] Yuefei Hu,[a] Wei He,[b] Linxing Zhang,*[c] Wenpeng Ma,*[d] and Kun An*[a]

The non-directed intermolecular C–H bond silylation has manifested itself as a versatile tool for the access of organosilicon compounds, however the corresponding asymmetric transformations remain elusive primarily due to the facile self-reactions of silane reactants. Herein we disclose an efficient protocol that involves steric-hindrance enabled, Rh-catalyzed enantioselective intermolecular C–H bond silylation of simple arenes to deliver a broad array of Si-stereogenic monohydrosilanes in good yields with excellent enantioselectivities (up to 99% ee), featuring readily available starting materials, simple synthetic operations and mild reaction conditions.

Introduction

The direct transformation of inexpensive, bulk chemicals into value-added products via C–H bond functionalization under mild conditions represents a longstanding goal in synthetic chemistry.[1-10] Particularly, the non-directed intermolecular C–H silylation has attracted considerable interest from both industrial and academic communities, owing to the broad utility of organosilicon compounds across materials science, organic synthesis, and pharmaceutical chemistry.[11-19] Despite efficient conversion of alkyl/aryl C–H bonds into C–Si bonds has seen major advances,[11-13] the development of corresponding asymmetric variants that forge carbon- or silicon-stereogenic centers remains in its infancy (**Scheme 1a**).[20] This scarcity stems primarily from a pronounced reactivity mismatch between the inert C–H bonds and the relatively more labile C–Si or Si–H bonds, which favors self-reactions of silane reactants over interception by C–H bond partners. Such challenge is further exemplified in the intermolecular dehydrogenative coupling of prochiral dihydrosilanes with simple arenes, the most straightforward and atom-economical route to Si-stereogenic monohydrosilanes, which have found versatile applications as mechanistic probe, bioactive molecule, and CPL-active material.[21-30] However, this route is often compromised by competing, entropy-driven silane redistribution arising from the formation of volatile silane byproducts.[31-40] Such challenge has largely restricted the available choice to heteroarenes, in which the α-C–H sites exhibit enhanced reactivity.[41-42] Although the mechanism of the side reaction is not fully understood, the concomitant cleavage of Si–C and Si–H bonds unequivocally lead to complex mixtures. We envision that suppressing C–Si bond activation by increasing steric hindrance around the silicon center might divert selectivity toward Si–H activation,[43-45] thereby enabling intermolecular C–H silylation in the presence of unactivated arenes. Building on our previous work in enantioselective C–H silylation of thiophenes using silacyclobutane as the silylation reagent,[46] herein we report a more challenging, Rh-catalyzed, enantioselective, and non-directed intermolecular C–H silylation of simple arenes, providing direct access to a wide range of Si-stereogenic diarylsilanes in good yields and with excellent enantioselectivities (**Scheme 1b**).

Results and discussion

We commenced our verification by reacting prochiral dihydrosilane **1** with 1,4-difluorobenzene under the catalysis of $[Rh(cod)Cl]_2$/(*R*)-DTBM-Segphos, a catalytic system proven effective in our prior intramolecular C–H silylation studies.[47] However, even under neat conditions, dihydrosilanes **1a-1b** predominantly yielded the redistribution byproducts **3a-3b** in 73~86% yield, with no detectable formation of the desired cross-coupled products. We therefore hypothesized that further augmenting steric hindrance on silicon might reverse the selectivity. Consistent with this premise, dihydrosilane **1c** bearing bulky cyclohexyl substituent reacted smoothly to give **2c** in 57% yield, albeit with no enantiocontrol (0% ee). Fortunately, the introduction of an additional *ortho*-substituent on the phenyl ring (**1d**) induced a pronounced shift in both chemoselectivity and enantioselectivity, cleanly furnishing the

[a] MOE Key Laboratory of Functional Molecular Solids, Anhui Basic Discipline Research Center for Clean Energy and Catalysis, College of Chemistry and Materials Science, Anhui Normal University, Wuhu 241002, China
[b] MOE Key Laboratory of Bioorganic Phosphorus Chemistry & Chemical Biology and School of Pharmaceutical Sciences, Tsinghua University, Beijing 100084, China
[c] College of Chemistry and Chemical Engineering, Hubei University, Wuhan 430062, China
[d] COFCO Nutrition & Health Research Institute Co. Ltd, Beijing 102209, China
† L. L., X. C. and G. G. contributed equally to this work.

View Article Online
DOI: 10.1039/D6SC01404E

enantioenriched monohydrosilane **2d** in 77% yield with 97% ee (**Scheme 2**). To further demonstrate the synergistic effect of *ortho*-OEt and *ortho*-Me substituents on steering chemoselectivity toward intermolecular C–H silylation, we conducted additional control experiments using benzene as the coupling partner to decouple electronic and steric contributions (see Supporting Information for details).

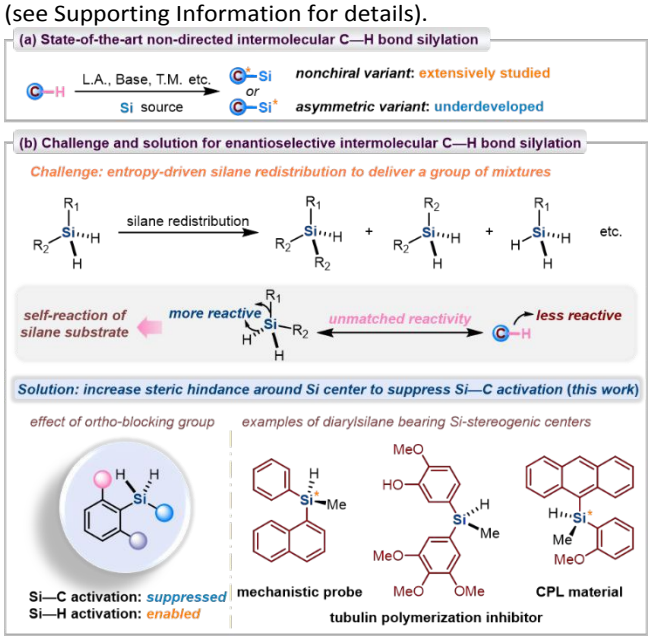

Scheme 1. Undirected intermolecular C–H bond silylation for the synthesis of diarylsilanes bearing Si-stereogenic centers.

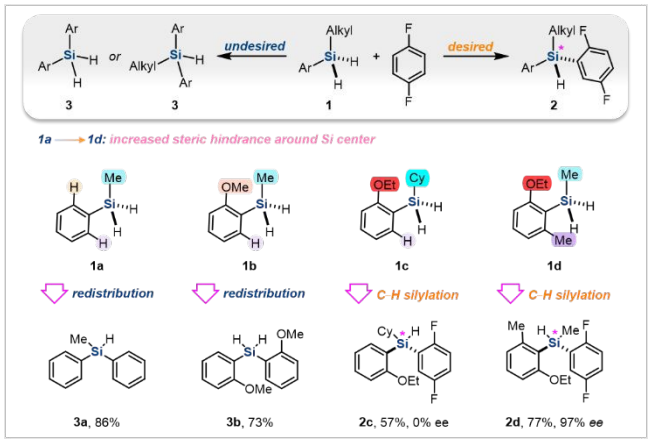

Scheme 2. Enantioselective intermolecular C–H bond silylation of 1,4-difluorobenzene. Reaction condition: dihydrosilane **1** (0.2 mmol), 1,4-difluorobenzene (neat, 2.0 mL), $[Rh(cod)Cl]_2$ (1.5 mol%), (*R*)-DTBM-segphos (3 mol%) at room temperature for 24 h. Isolated yields were given and the ee value was determined by chiral HPLC analysis.

Encouraged by the above preliminary results, we then undertook a comprehensive optimization of the reaction parameters (**Table 1**). Our investigation began with a systematic evaluation of chiral bisphosphine ligands for the benchmark reaction of **1d** with 1,4-difluorobenzene under neat conditions (entry 1 - 8). A clear structure-activity relationship emerged as ligands with substantial steric hindrance (**L4**, **L7**, and **L8**) consistently delivered good yields and enantioselectivities, whereas their less hindered counterparts (**L1**, **L2**, **L3**, **L5** and **L6**) afforded only trace product. Among the effective ligands, **L7** was identified to provide the highest enantiomeric purity (97% ee). Subsequent screening of the rhodium catalysts showed that $[Rh(NBD)Cl]_2$ outperformed $[Rh(cod)Cl]_2$, increasing the yield of **2d** to 85% without eroding enantiocontrol (entry 9). The reaction efficiency was further probed by reducing the amount of 1,4-difluorobenzene to 10 equivalents (entry 10). This modification left the enantioselectivity unaffected but led to a decrease in yield, accompanied by incomplete consumption of the starting material. Considering a balance between efficiency and practicality, the optimal conditions were defined as follows: $[Rh(NBD)Cl]_2$ (1.5 mol%), (*R*)-DTBM-Segphos (3 mol%), in neat arenes, at room temperature for 24 h.

Table 1. Optimization of reaction conditions.

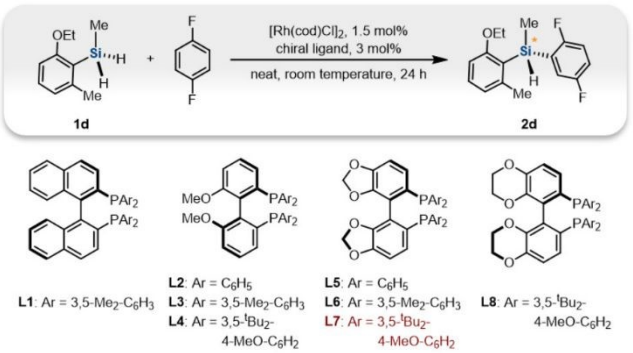

Entry	Ligand	Yield of 2d/%	ee of 2d/%
1	L1	trace	-
2	L2	trace	-
3	L3	trace	-
4	L4	60	93
5	L5	trace	-
6	L6	trace	-
7	L7	77	97
8	L8	62	90
9[a]	L7	85	97
10[b]	L7	58	97

Reaction conditions: **1d** (0.2 mmol), 1,4-difluorobenzene (neat, 2.0 mL), $[Rh(cod)Cl]_2$ (1.5 mol%), chiral ligand (3 mol%) at room temperature for 24 h. Isolated yields were given and the ee values were determined by chiral HPLC analysis. [a]$[Rh(NBD)Cl]_2$ was used as catalyst. [b]A mixed solvent was employed (hexane: 1.0 mL, 1,4-difluorobenzene: 0.2 mL).

With the optimized conditions in hand, we then evaluated the substrate scope of simple arenes under neat conditions (**Scheme 3**). This protocol proved robust in delivering the targeted Si-stereogenic monohydrosilanes **2d-2q** in moderate to high yields (51~93%) with consistently excellent enantioselectivities (76~99% ee). A key observation was that enantioselectivity remained uniformly high and was insensitive to variations in the electronic properties or steric demand of the substituents. In contrast, regioselectivity was strongly sterically dependent: di- and multi-substituted arenes (**2d–2j** and **2n**) exhibited high regioselectivity, whereas monosubstituted arenes (**2k–2m** and **2o–2p**) gave mixtures of regioisomers. We propose that the observed regioselectivity is governed by a combination of steric and electronic effects. For substrates in which the reactive sites are sterically differentiated, regioselectivity is predominantly dictated by steric repulsion from the substituents. The bulkier groups effectively shield one potential reaction site, directing the transformation to the more accessible position. In contrast, for substrates that possess multiple less hindered sites with comparable steric

environments, electronic effects emerge as the key factor governing regioselectivity. In these cases, the intrinsic electronic bias of the substrate dictates the preferential activation of one site over others. Besides, the absolute ***S*** configuration of a representative product, **2d**, was unambiguously confirmed by single-crystal *X-ray* diffraction analysis.

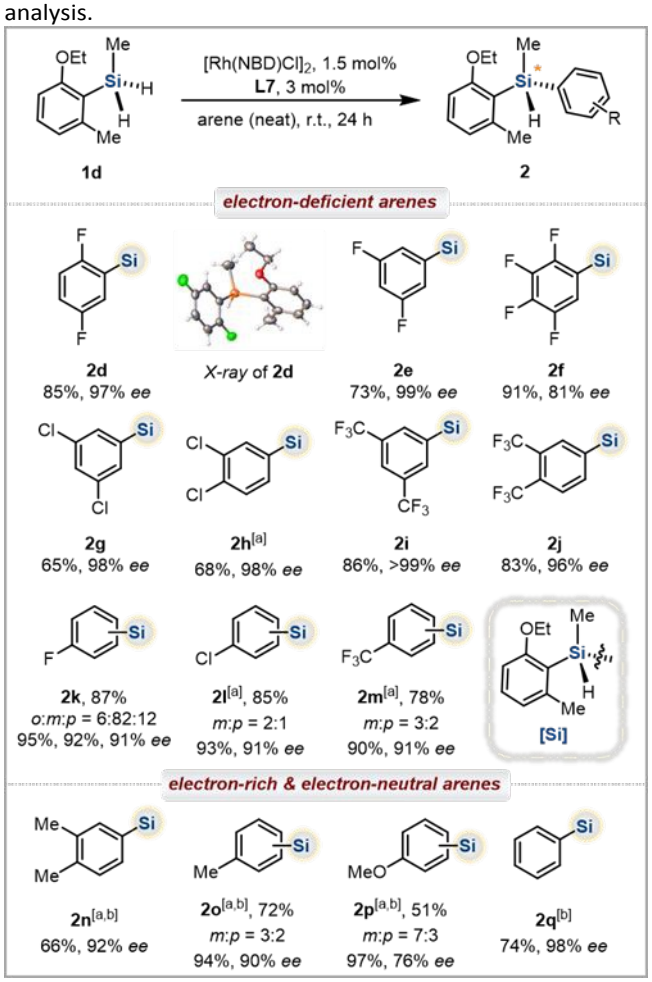

Scheme 3. Scope of simple arenes. Reaction conditions: **1d** (0.2 mmol), arene (neat, 2.0 mL), $[Rh(NBD)Cl]_2$ (1.5 mol%), (*R*)-DTBM-segphos (3 mol%), at room temperature for 24 h. Isolated yields were given and the *ee* values were determined by chiral HPLC analysis. [a]at 65 °C for 48 h. [b]$[Rh(NBD)Cl]_2$ (3 mol%), (*R*)-DTBM-segphos (6 mol%), at room temperature for 48 h.

Having demonstrated the scope of arenes, we next evaluated a range of dihydrosilanes under analogous conditions (**Scheme 4**). These substrates were successfully converted into diarylsilanes bearing Si-stereogenic centers, using 1,4-difluorobenzene as the representative coupling partner. By strategically modulating the alkoxy and alkyl substituents on silicon, unwished C–Si bond cleavage was effectively suppressed. Consequently, the reactions of **1r-1w** proceeded efficiently, affording the corresponding enantioenriched monohydrosilanes in high yields (80~88%) with excellent enantioselectivities (88~98% ee). Notably, the sterically demanding 2,6-dimethylphenyl-substituted dihydrosilane **1x** was also compatible, delivering **2x** in good yield (78%) with moderate enantioselectivity (69% ee). This result implies that the *ortho*-OEt group might play a unique synergistic role, combining optimal steric demand with potential coordinative effects to achieve both high chemoselectivity and exceptional enantioselectivity. To further elucidate this phenomenon, additional control experiments were performed, and a similar trend was revealed (see Supporting Information for details). Moreover, the absolute configuration of **2w** was unequivocally determined to be ***S*** by single-crystal *X-ray* diffraction analysis.

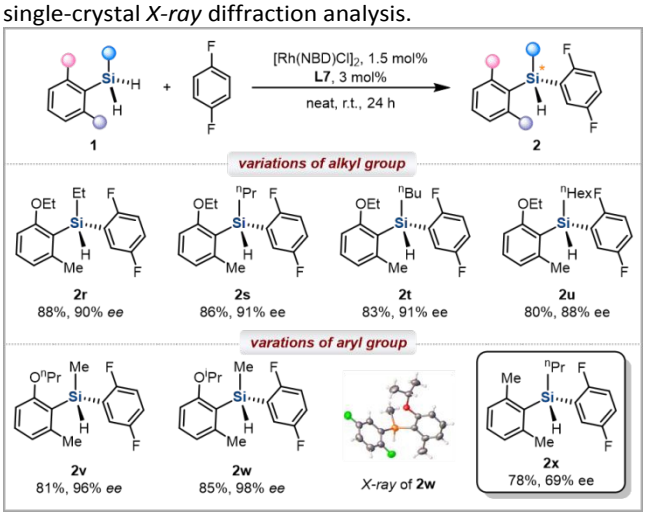

Scheme 4. Scope of dihydrosilanes. Reaction conditions: dihydrosilane **1** (0.2 mmol), 1,4-difluorobenzene (neat, 2.0 mL), $[Rh(NBD)Cl]_2$ (1.5 mol%), (*R*)-DTBM-segphos (3 mol%), at room temperature for 24 h. Isolated yields were given and the *ee* values were determined by chiral HPLC analysis.

To highlight the practical utility of this method, the reaction between **1d** and 1,4-difluorobenzene was performed on a preparative scale, providing **2d** in undiminished yield and enantioselectivity (**Scheme 5a**). The versatility of the enantioenriched monohydrosilane was then demonstrated via two distinct late-stage transformations, enabling access to diverse chiral tetraorganosilicon architectures (**Scheme 5b**): Dehydrogenative coupling of the Si–H moiety in **2d** with BnOH furnished **2y** in 89% yield with full preservation of enantiopurity (96% ee). Alternatively, Karstedt's catalyst promoted hydrosilylation delivered adduct **2z** in 56% yield, albeit with a modest reduction in enantiomeric excess (89% ee).

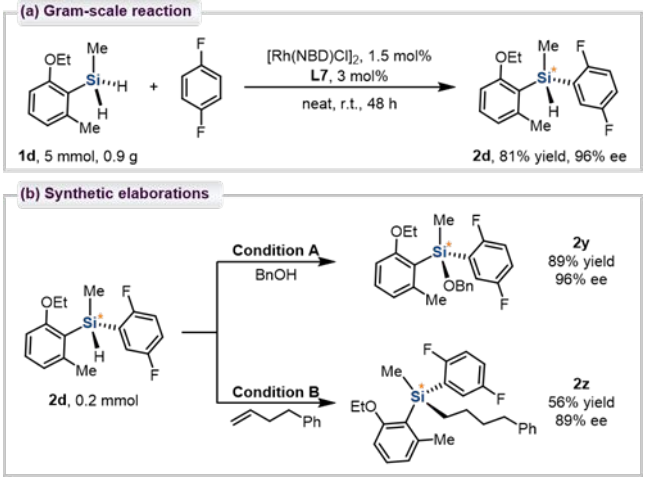

Scheme 5. Scaled-up reaction and synthetic elaborations. Condition A: CuCl (10 mol%), (*R,R*)-Ph-BPE (11 mol%), ^{t}BuONa (10 mol%), **2d** (0.2 mmol), BnOH (0.3 mmol, 1.5 equiv.), toluene (2.0 mL), at 30 °C for 24 h. Condition B:

View Article Online
DOI: 10.1039/D6SC01404F

Pt(dvds) (5 mol%), **2d** (0.2 mmol), alkene (0.4 mmol, 2.0 equiv.), cyclohexane (2.0 mL), 65 °C for 24 h.

To gain further insight into the reaction mechanism, deuterated reactant **D-1d** was prepared and kinetic studies were conducted (**Scheme 6a**). Parallel reactions employing isotopically labeled substrates revealed distinct kinetic isotope effects (KIEs). A small KIE (~1/1) was obtained from competition between **D-1d** and **1d** in benzene, whereas a significantly larger KIE (~4/1) was observed when comparing reactions of **1d** in benzene versus perdeuterated benzene. These results collectively suggest that cleavage of the arene C–H bond, rather than the Si–H bond, is likely involved in the rate-limiting step.

Integrating these preliminary results with literature precedents,[48-49] we propose a plausible catalytic cycle as illustrated in **Scheme 6b**. The cycle is initiated by the in situ generation of a rhodium hydride species, followed by coordination of the ethereal oxygen atom of the *ortho*-OEt group to the rhodium center prior to the oxidative addition step. This coordination effectively transforms what would otherwise be an intermolecular Si–H bond oxidative addition into a formal intramolecular process. Oxidative addition of **A** into the less sterically hindered Si–H bond then occurs to yield intermediate **B**, accounting for the observed high enantioselectivity. Subsequent reductive elimination from **B** affords the rhodium–silicon species **C** with concomitant release of H_2. Species **C** then undergoes oxidative addition into the C–H bond of the neat arenes to give intermediate **D**. Finally, reductive elimination of **D** delivers the resulting Si-stereogenic monohydrosilane and regenerates the active rhodium hydride catalyst.

To validate the proposed role of *ortho*-OEt group and elucidate the origin of enantioselectivity, density functional theory (DFT) calculations were performed on the Si–H oxidative addition step of **1d** (**Scheme 6c**) in benzene. The results revealed that the formation of (*R*)-**2q** via **TS1-*R*** is kinetically favored over the formation of (*S*)-**2q** via **TS1-*S*** by 3.4 kcal mol^{-1}, consistent with the experimentally observed stereoselectivity. Notably, both transition states feature comparable Rh–O interactions, providing computational support for the proposed coordination of the *ortho*-OEt group to the rhodium center. The resulting conformational restriction enhances steric differentiation between **TS1-*R*** and **TS1-*S***, with **TS1-*S*** experiencing greater steric repulsion between the silyl methyl group and the chiral ligand. Furthermore, additional DFT calculations were conducted to investigate the competing oxidative addition pathways of **1d** (Si–Me and Si–Ar activation), and the calculated chemoselectivity is in good agreement with the experimental findings (see Supporting Information for details).

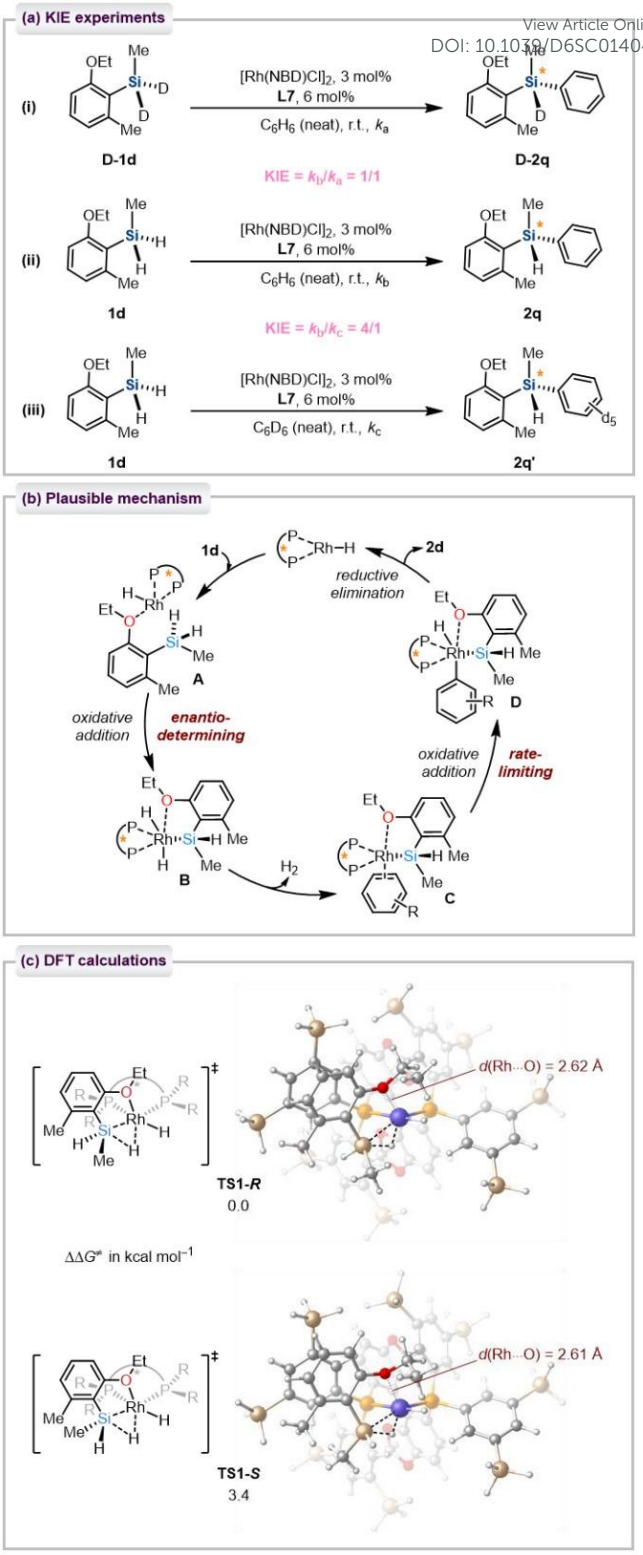

Scheme 6. Kinetic isotope effect studies, plausible mechanism and DFT calculations.

Conclusions

To sum up, we have developed an efficient and highly enantioselective method for the non-directed intermolecular C–H bond silylation of simple arenes with prochiral

View Article Online
DOI: 10.1039/D6SC01404H

dihydrosilanes. This work establishes an unprecedented protocol for the direct conversion of simple arenes into value-added Si-stereogenic monohydrosilanes in high yield with excellent enantioselectivity. Our systematic investigation identified and overcame silane redistribution as a major challenge, which was effectively suppressed through strategic selection of dihydrosilane substrates and chiral ligands. We reckon that future advances in ligand design will broaden the current substrate scope. Related studies, including a full mechanistic investigation, are underway in our laboratory and shall be disclosed in due course.

Author contributions

L. L., X. C., G. G., X. S. and M. L. conceptualized the research and performed the investigation. Y. H. and W. H. analysed the data and provided valuable suggestions. L. Z. conducted the DFT calculations. K. A. wrote the manuscript with contributions from all authors. L. Z., W. M. and K. A. supervised this study.

Conflicts of interest

There are no conflicts to declare.

Data availability

All the data supporting this article have been included in the main text and the supplementary information. CCDC **2126543** (**2d**), **2126544** (**2w**) contains the supplementary crystallographic data for this paper. These data can be obtained free of charge via www.ccdc.cam.ac.uk/data_request/cif, or by emailing data_request@ccdc.cam.ac.uk, or by contacting The Cambridge Crystallographic Data Centre, 12 Union Road, Cambridge CB2 1EZ, UK; fax: +44 1223 336033.

Acknowledgements

This work was supported by the National Natural Science Foundation of China (No. 21971133, 22403028), the National Key Research and Development Program of China (2017YFA0505203) and the start-up fund of Anhui Normal University (903-762318, 114-022304).

Notes and references

1 N. Y. S. Lam, K. Wu, J.-Q. Yu, *Angew. Chem. Int. Ed*., 2021, **60**, 15767–15790.
2 L. Guillemard, N. Kaplaneris, L. Ackermann, M. J. Johansson, *Nat. Rev. Chem*., 2021, **5**, 522–545.
3 S. K. Sinha, S. Guin, S. Maiti, J. P. Biswas, S. Porey, D. Maiti, *Chem. Rev*., 2022, **122**, 5682–5841.
4 L. Zhang, T. Ritter, *J. Am. Chem. Soc*., 2022, **144**, 2399–2414.
5 P. Bellotti, H.-M. Huang, T. Faber, F. Glorius, *Chem. Rev*., 2023, **123**, 4237–4352.
6 J. H. Docherty, T. M. Lister, G. McArthur, M. T. Findlay, P. Domingo-Legarda, J. Kenyon, S. Choudhary, J. Larrosa, *Chem. Rev.*, 2023, **123**, 7692–7760.
7 C.-X. Liu, S.-Y. Yin, F. Zhao, H. Yang, Z. Feng, Q. Gu, S.-L. You, *Chem. Rev*., 2023, **123**, 10079–10134.
8 Y. Zhang, J.-J. Zhang, L. Lou, R. Lin, N. Cramer, S.-G. Wang, Z. Chen, *Chem. Soc. Rev*., 2024, **53**, 3457–3484.
9 C. Romano, R. Martin, *Nat. Rev. Chem.*, 2024, **8**, 833–850.
10 N. R. Ciccia, J. F. Hartwig, *Angew. Chem. Novit*, 2025, **1**, e70013.
11 S. C. Richter, M. Oestreich, *Trends Chem*., 2020, **2**, 13–27.
12 B. Li, P. H. Dixneuf, *Chem. Soc. Rev.*, 2021, **50**, 5062–5085.
13 I. F. Yu, J. W. Wilson, J. F. Hartwig, *Chem. Rev.*, 2023, **123**, 11619–11663.
14 B. A. Kamino, T. P. Bender, *Chem. Soc. Rev.*, 2013, **42**, 5119–5130.
15 Y. Zuo, Z. Gou, W. Quan, W. Lin, *Coord. Chem. Rev*., 2021, **438**, 213887.
16 R. Ramesh, D. S. Reddy, *J. Med. Chem.*, 2018, **61**, 3779–3798.
17 G. Luo, L. Chen, Y. Li, Y. Fan, D. Wang, Y. Yang, L. Gao, R. Jiang, Z. Song, *Org. Chem. Front*., 2021, **8**, 5941–5947.
18 J.-L. Panayides, D. L. Riley, F. Hasenmaile, W. A. L. Van Otterlo, *RSC Med. Chem*., 2024, **15**, 3286–3344.
19 T. Komiyama, Y. Minami, T. Hiyama, *ACS Catal*., 2017, **7**, 631–651.
20 Y. Ge, X. Huang, J. Ke, C. He, *Chem Catal.*, 2022, **2**, 2898–2928.
21 F. Ye, Z. Xu, L.-W. Xu, *Acc. Chem. Res*., 2021, **54**, 452–470.
22 Y. Wu, P. Wang, *Angew. Chem. Int. Ed*., 2022, **61**, e202205382.
23 L. Li, W.-S. Huang, Z. Xu, L.-W. Xu, *Sci. China Chem.*, 2023, **66**, 1654–1687.
24 Y. Wu, L. Zheng, Y. Wang, P. Wang, *Chem*, 2023, **9**, 3461–3514.
25 Y. Ge, J. Ke, C. He, *Acc. Chem. Res.*, 2025, **58**, 375–398.
26 L. H. Sommer, C. L. Frye, *J. Am. Chem. Soc.*, 1959, **81**, 1013–1013.
27 Y. Kurihara, M. Nishikawa, Y. Yamanoi, H. Nishihara, *Chem. Commun*. 2012, **48**, 11564–11566.
28 L. Chen, J.-B. Huang, Z. Xu, Z.-J. Zheng, K.-F. Yang, Y.-M. Cui, J. Cao, L.-W. Xu, *RSC Adv*., 2016, **6**, 67113–67117.
29 S. Koga, S. Ueki, M. Shimada, R. Ishii, Y. Kurihara, Y. Yamanoi, J. Yuasa, T. Kawai, T.-A. Uchida, M. Iwamura, K. Nozaki, H. Nishihara, *J. Org. Chem*., 2017, **82**, 6108–6117.
30 M. Nakamura, D. Kajita, Y. Matsumoto, Y. Hashimoto, *Bioorg. Med. Chem.*, 2013, **21**, 7381–7391.
31 M. D. Curtis, P. S. Epstein, *Adv. Organomet. Chem*., 1981, **19**, 213–255.
32 S. Park, B. G. Kim, I. Göttker-Schnetmann, M. Brookhart, *ACS Catal*., 2012, **2**, 307–316.
33 Y. Ma, L. Zhang, Y. Luo, M. Nishiura, Z. Hou, *J. Am. Chem. Soc*., 2017, **139**, 12434–12437.
34 X. Liu, L. Xiang, E. Louyriac, L. Maron, X. Leng, Y. Chen, *J. Am. Chem. Soc.*, 2019, **141**, 138–142.
35 Y. Chen, L. Ai, Y. Li, C. Xu, *RSC Adv*., 2020, **10**, 17404–17407.
36 C. Guo, M. Li, J. Chen, Y. Luo, *Chem. Commun.*, 2020, **56**, 117–120.
37 T. Li, K. N. McCabe, L. Maron, X. Leng, Y. Chen, *ACS Catal.*, 2021, **11**, 6348–6356.
38 S. Chen, X. He, C. Jin, W. Zhang, Y. Yang, S. Liu, Y. Lan, K. N. Houk, X. Shen, *Angew. Chem. Int. Ed*., 2022, **61**, e202213431.
39 N. Swann, K. Tang, J. Nam, J. Lee, M. Domin, T. E. Shaw, S. A. Kozimor, S. Som, K. L. Lee, *Chem. Sci.*, 2024, **15**, 11912–11918.
40 J. Zhang, X. Tian, Y. Wang, Y. Zhang, F. Wang, L. Wu, *J. Am. Chem. Soc.*, 2024, **146**, 33349–33358.
41 S. Chen, J. Zhu, J. Ke, Y. Li, C. He, *Angew. Chem. Int. Ed.*, 2022, **61**, e202117820.
42 D. Mu, S. Pan, X. Wang, X. Liao, Y. Huang, J. Chen, *Chem. Commun*., 2022, **58**, 7388–7391.
43 H. Wen, X. Wan, Z. Huang, *Angew. Chem. Int. Ed*. 2018, **57**, 6319–6323.

View Article Online
DOI: 10.1039/D6SC01404F

44 T. He, L.-C. Liu, W.-P. Ma, B. Li, Q.-W. Zhang, W. He, *Chem. Eur. J*. 2020, **26**, 17011–17015.
45 J.R. Jagannathan, J.C. Fettinger, J.T. Shaw, A.K. Franz, *J. Am. Chem. Soc*. 2020, **142**, 11674–11679.
46 K. An, W. Ma, L.-C. Liu, T. He, G. Guan, Q.-W. Zhang, W. He, *Nat. Commun.*, 2022, **13**, 847.
47 W. Ma, L.-C. Liu, K. An, T. He, W. He, *Angew. Chem. Int. Ed.*, 2021, **60**, 4245–4251.
48 L. Zhang, K. An, Y. Wang, Y.-D. Wu, X. Zhang, Z.-X. Yu, W. He, *J. Am. Chem. Soc.*, 2021, **143**, 3571–3582.
49 N. Li, J. Ke, L.-Q. Ren, Y. Li, C. He, *Chem Catal*., 2023, **3**, 100799.

View Article Online
DOI: 10.1039/D6SC01404F

Data availability

All the data supporting this article have been included in the main text and the supplementary information. CCDC **2126543** (**2d**), **2126544** (**2w**) contains the supplementary crystallographic data for this paper. These data can be obtained free of charge via www.ccdc.cam.ac.uk/data_request/cif, or by emailing data_request@ccdc.cam.ac.uk, or by contacting The Cambridge Crystallographic Data Centre, 12 Union Road, Cambridge CB2 1EZ, UK; fax: +44 1223 336033.